Journal of Power Sources 301 (2016) 317–325

Contents lists available at ScienceDirect

Journal of Power Sources

journal homepage: www.elsevier.com/locate/jpowsour

Immobilized transition metal-based radical scavengers and their effect on durability of Aquivion® perfluorosulfonic acid membranes

C. D'Urso [a], C. Oldani [b], V. Baglio [a, *], L. Merlo [b], A.S. Aricò [a]

[a] Istituto di Tecnologie Avanzate per l'Energia "Nicola Giordano" (CNR), Via Salita S. Lucia sopra Contesse, 5, 98126 Messina, Italy
[b] Solvay Specialty Polymers Italy S.p.A., Viale Lombardia 20, Bollate, MI, Italy

HIGHLIGHTS

- Silica-supported transition metal-based radical scavengers are prepared.
- The scavengers contain sulfonic acid functionalities.
- The scavenger was loaded in ePTFE reinforced Aquivion® membranes.
- All composite membranes show longer lifetime than the scavenger-free membranes.
- The Cr-based membrane shows a 3-time larger stability than pristine membranes.

ARTICLE INFO

Article history:
Received 21 May 2015
Received in revised form
11 September 2015
Accepted 7 October 2015

Keywords:
Polymer electrolyte membrane
Composite membrane
Radical scavenger
Accelerated stress test
Aquivion® PFSA

ABSTRACT

A simple and broadly applicable preparation procedure to obtain silica-supported transition metal (namely Cr, Co and Mn)-based radical scavengers, containing sulfonic acid functionalities, is reported. These systems are widely characterised in terms of structure, bulk and surface composition and morphology by X-Ray Diffraction (XRD), X-Ray Fluorescence (XRF), X-Ray Photoelectron Spectroscopy (XPS) and Transmission Electron Microscopy (TEM). The scavenger material is loaded in ePTFE reinforced membranes prepared from Aquivion® perfluorosulfonic acid (PFSA) dispersions. All these composite membranes show longer lifetime in Accelerated Stress Tests (AST) and reduced fluoride release in Fenton's tests than the scavenger-free membranes without any loss in electrochemical performance. The Cr-scavenger-based polymer electrolyte shows a three-time larger stability than the pristine membrane.

1. Introduction

Thanks to their high energy conversion efficiency, hydrogen-fed fuel cells (FCs) are today widely considered as one of the most environmental-friendly power sources. They are attracting interest as one of the potential solutions to mitigate global pollution, reduce fossil fuels dependence and address increased energy demand [1]. Today fuel cells find application in automotive, stationary and backup power generation [2].

The membrane plays a key role in polymer electrolyte membrane fuel cells (PEMFCs) not only because it is the core part of these devices, transporting protons between the electrodic compartments, but it keeps fuel and oxidant separate and, being an electron insulator, avoids electron drag through the electrolyte and thus forces electrons to flow in the external circuit generating the electric current [3,4].

In the last years, many different ionomers (*i.e* polymers bearing ionic charges) have been developed, and, in several cases, used to prepare membranes now available on the market [5]. These polymers can be roughly classified as fully hydrogenated [6] (such as sulfonated polystyrene and polyether ether ketone), partially fluorinated [7] and perfluorinated, also known as PerFluoroSulfonic Acid (PFSA) [8].

Among the others perfluorinated and commercially available ionomer membrane, Aquivion® PFSA [9] (marketed by Solvay Specialty Polymers), thanks to its short side chain, shows very peculiar and valuable properties such as high performance at elevated temperature and low humidity level [10–12]. Moreover, when compared to conventional long side chain Nafion®, the presence of only one ether group and the absence of the tertiary

* Corresponding author.
E-mail address: baglio@itae.cnr.it (V. Baglio).

http://dx.doi.org/10.1016/j.jpowsour.2015.10.019
0378-7753/

carbon provide Aquivion® PFSA with longer durability also in very harsh operating conditions [13].

Membrane durability is a very important factor to achieve an appropriate PEMFC lifetime. Membrane degradation during operation in FCs, in general, is related both to mechanical stress and chemical degradation [14,15]. The former is associated to compression-tension induced by repetitive membrane swelling-shrinkage triggered by relative humidity and temperature variations, whereas the latter is believed to be initiated by the formation, both at the cathode and at the anode side, of strongly reactive radical species such as hydroxy (HO*), hydroperoxy (HOO*) and hydrogen (H*) radicals [16–18]. Although the lack of general agreement about the involved decay mechanisms, chemical radicals are considered responsible of the PFSA degradation at the backbone as well as at the side chain level leading to membrane failure [19,20].

In order to minimize degradation and increase membrane lifetime, several approaches have been proposed such as the development of chemically stabilized and low gas-crossover membranes as well as the incorporation of hydrogen peroxide decomposition catalysts and radical scavengers [21]. It has been already reported by many Authors that, for example, Cerium and Manganese derivatives (metal oxides [22–25], metal nanoparticles [24] or respective ions [26,27]) also immobilized onto inert supports [28] are effective as radical scavengers and their introduction leads to a significant increase in PEMFC lifetime.

The radical scavenging activity (*i.e.* the ability to catalytically transform highly reactive, aggressive peroxides into inert species) of transition metals is related to both kinetics and thermodynamics aspects. One speculative hypothesis relies on the fact that transition metals can interact with peroxy-radicals especially if they are characterised by oxidation states with redox potentials closely matching those of the radicalic species. In this regard, it is interesting to evaluate the behaviour of radical scavengers based on transition metals with different chemistries and oxidation states.

In this contribution, we report a straightforward and broadly applicable preparation procedure to obtain silica-supported transition metal (namely Cr, Co and Mn)-based radical scavengers. Silica was selected as a support due to its high surface area and the presence of a large number of hydroxyl (−OH) groups, which can be further functionalized. Furthermore, silica is widely used as a filler in fuel cell membranes, as reported in several papers [29–31], and in combination with PFSA in heterogeneous acid catalysis [32,33].

The prepared silica-supported transition metal-based radical scavengers have been widely characterised and incorporated in short side chain Aquivion® PFSA membranes. The evaluation of membrane durability has been assessed by *ex-situ* Fenton's test as well as *in-situ* Accelerated Stress Tests (AST).

2. Experimental

M-oxide (with M=Cr, Co and Mn) scavengers supported on silica and containing sulfonic species were synthesized using a procedure reported in Ref. [28]. A simple wet impregnation technique was employed. In a closed vessel SiO_2 (EH5 from Cabot), $M(NO_3)_3{}^*6H_2O$ and $(NH_4)_2SO_3{}^*H_2O$ were suspended in water. The reactant wt. ratio was silica:M-salt:$(NH_4)_2SO_3{}^*H_2O$ = 8:1.5:0.5. The slurry was stirred at 80 °C for 16 h until a gel was obtained. This was heated from room temperature to 150 °C in 1 h, maintained constant at 150 °C for 2 h, then heated from 150 °C to 300 °C in 1 h and kept constant at 300 °C for 2 h. The obtained powder was cooled down from 300 °C to room temperature in 1 h. The specific thermal treatment was a key aspect to achieve the desired dispersion properties for metallic species and to promote anchoring of sulphur moieties on the sample surface. The powder was then washed with 0.5 M H_2SO_4 solution at 70 °C until X-Ray Fluorescence (XRF) of the collected solutions from sample washing showed no change in the amount of metal and sulphur. The material was dried under vacuum at 80 °C for 2 h and then ground in a planetary ball mill for 2 h at 200 rpm.

XRF analysis of the scavengers was carried out by a Bruker AXS S4 Explorer spectrometer to determine the elemental composition of the as prepared sample and after washing with diluted sulphuric acid solution. X-Ray diffraction (XRD) powder patterns for the materials were obtained on a Philips X'Pert X-ray diffractometer using a Cu/Kα source operating at 40 kV and 30 mA. Transmission Electron Microscopy (TEM) analysis was carried out by first dispersing the samples in isopropyl alcohol. A few drops of these solutions were deposited on carbon film-coated Cu grids and analyzed with a FEI CM12 microscope.

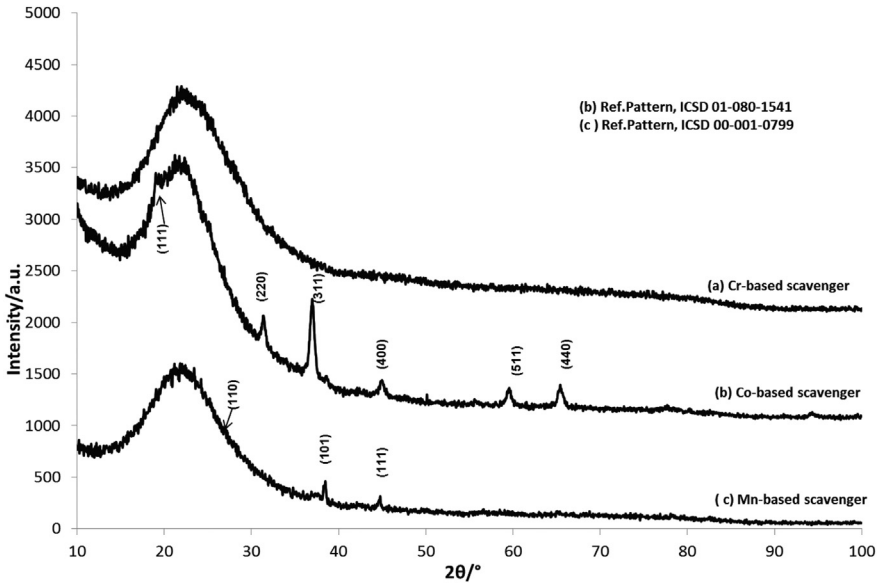

Fig. 1. X-ray diffraction pattern of the different scavengers supported on sulfonated silica.

The surface chemical composition of the catalysts was investigated by X-ray Photoelectron Spectroscopy (XPS) using a Physical Electronics (PHI) 5800-01 spectrometer. A monochromatic Al Ka X-ray source was used at a power of 300 W. Spectra were obtained with a pass energy of 58.7 eV for elemental analysis (composition) and 11.75 eV for the determination of the chemical species. The pressure in the analysis chamber of the spectrometer was 1×10^{-9} Torr during the measurements.

The pH of a slurry composed of 0.1 g scavenger powder in 0.1 l of bi-distilled water was measured at room temperature by an ATC compensated pH probe (Orion).

In order to prepare the Aquivion® PFSA dispersion, transition-metal-oxide-based scavengers supported on silica (1 g) were suspended in 1-propanol (50 g); the mixtures were sonicated in an ultrasonic bath at room temperature for 2 h to obtain a complete dispersion of the solid. The amount of alcoholic dispersion required to obtain the desired radical scavenger loading was added dropwise to a stirred mixture of a commercially available water-based Aquivion® PFSA dispersion D79-25BS (100 g, equivalent weight: 790 g mol^{-1}, 25 wt% solid content, chemically stabilized in order to transform the residual carboxylic acid end groups into stable $-CF_3$), 1-propanol (36 g) and *N*-ethylpyrrolidinone (15.5 g). After 15 min of stirring at room temperature, a clear and transparent mixture was obtained. The same procedure was used for the ionomer solution not containing any scavenger.

For the preparation of reinforced membranes, an expanded PTFE support (Tetratex 3101 purchased from Donaldson Inc., USA) was mounted on a PTFE circular frame having an internal diameter of 100 mm and then was immersed in the ionomer mixture described above at room temperature for 2 min. The specimen was then heat treated in a vent oven at 65 °C for 1 h, at 90 °C for 1 h and from 90 °C to 190 °C in 1 h. The membranes thus obtained were transparent and colourless indicating the full and homogeneous occlusion of porous support with the ionomer. The thickness of the resulting membranes was 25 ± 2 μm.

The Fluoride Emission Rate (FER) of the radical scavenger-free reinforced membrane and the same including the different scavengers supported on silica was investigated by the Fenton's test. Pre-weighted membrane samples (0.3 g) were added to a plastic vessel equipped with a water cooled condenser and containing a solution of H_2O_2 (15 wt%, 200 g), $Fe(NH_4)_2(SO_4)_2{}^*6H_2O$ (0.05 g) and H_2SO_4 (0.5 M, 0.025 g). The system was allowed to react for 4 h at a constant temperature of 75 °C then the membrane sample was removed and the solution was cooled-down till room temperature. The aqueous medium was collected and fluoride concentration was measured *via* Ion-exchange Chromatography (IC) using a DIONEX ICS3000 chromatography system equipped with a DIONEX IONPACK AS14A anion-exchange column and an eluent generator providing a gradient elution from KOH/H_2O 10 mM to KOH/H_2O 70 mM.

Scavenger-free and scavenger-doped membranes were assembled with as-received carbon paper gas diffusion electrodes H400 (SolviCore GmbH & Co. KG, Germany) consisting of 0.5 mg cm^{-2} platinum loading. Each MEA was installed in a single cell triple serpentine flow field hardware (Fuel Cell Technologies, Inc., USA) with an active area of 25 cm^2. The MEAs were tested on a 50 W test stand (Arbin Instruments, USA). The MEA conditioning duration was 20 h; it was carried out as follows: 0.6 V cell potential, temperature of 75 °C, 80% relative humidity (RH), feeding H_2/air at 1 bar absolute (barA) pressure. Reported polarization curves were

Table 1
Composition of the scavengers supported on sulfonated silica determined by XRF.

Elements	Co-based scavenger (wt%)	Mn-based scavenger (wt%)	Cr-based scavenger (wt%)
Si	74.72	88.62	63.98
Metal	24.96	11.20	31.39
S	0.32	0.18	4.63

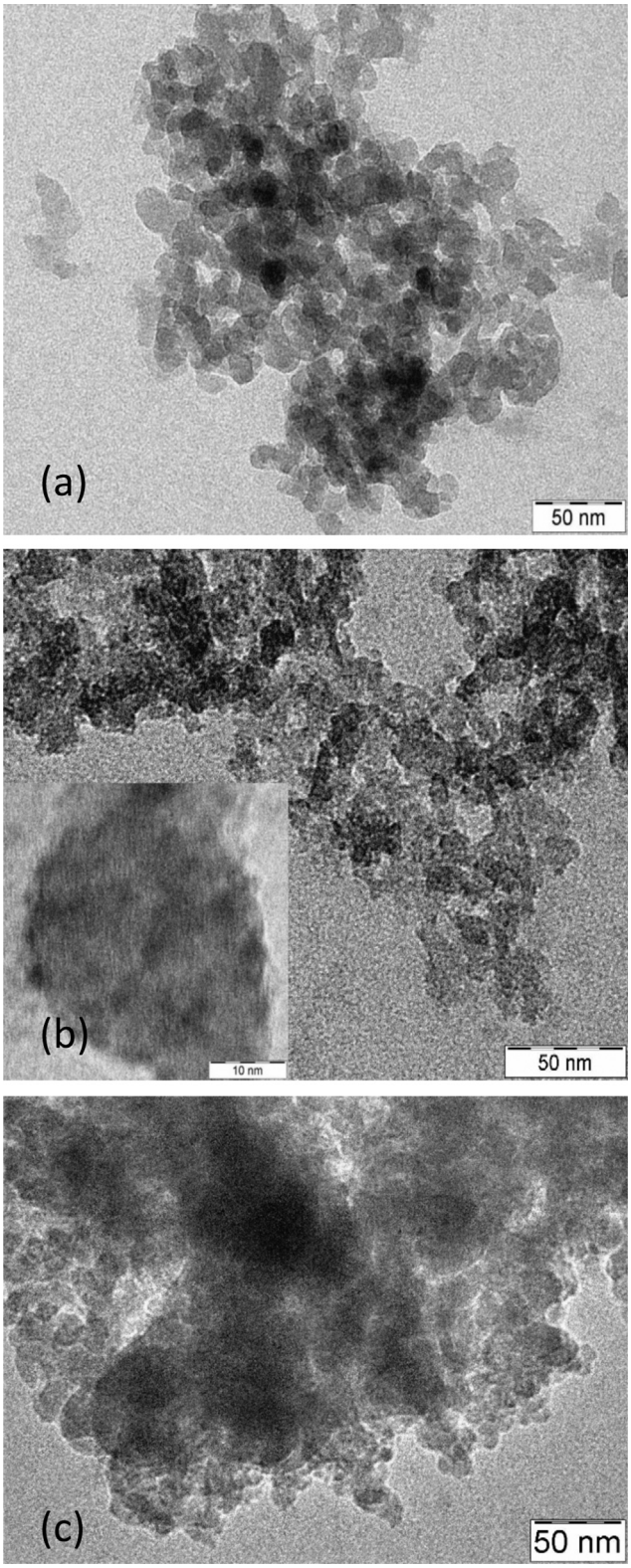

Fig. 2. TEM micrographs of (a) Mn-based, (b) Cr-based and (c) Co-based scavengers supported on sulfonated silica.

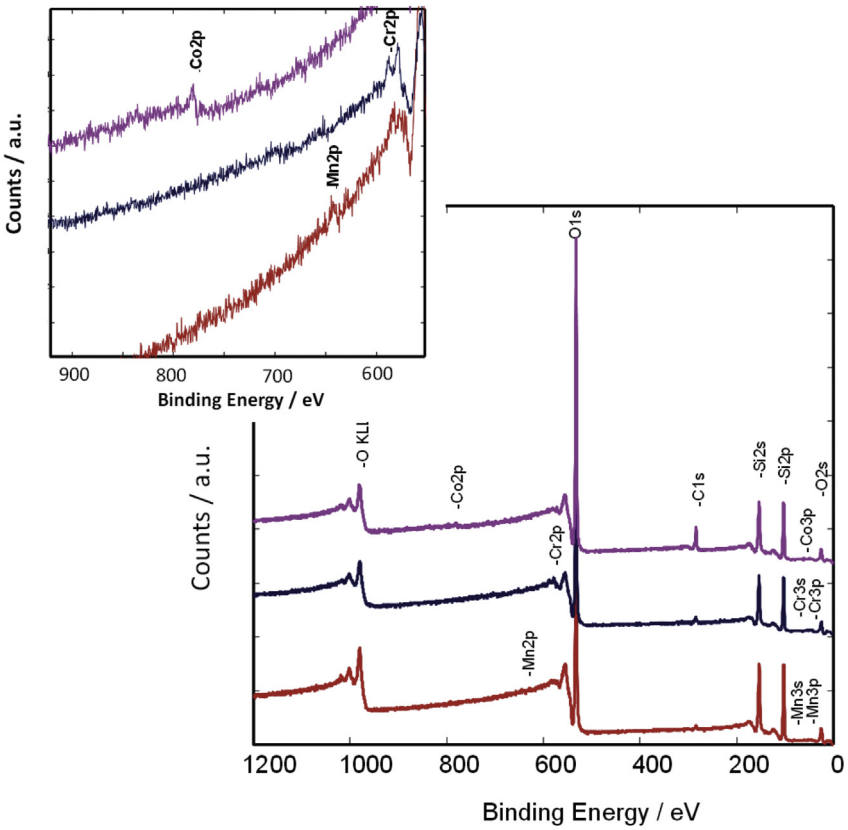

Fig. 3. XPS survey spectra of Mn-based, Cr-based and Co-based scavengers.

recorded at T: 75 °C, RH: 65%, P: 1 barA (either side) and feeding H_2/air. Accelerated Stress Tests (AST) were carried out at 90 °C, RH: 30%, P: 1 barA (either side), feeding H_2/O_2 in Open Circuit Voltage (OCV) condition and fixing the failure limit at 0.7 V. Each test was repeated at least twice. The stoichiometry ratio for H_2:air was fixed at 1:2 during the polarization curves for current density higher than 200 mA cm^{-2}. The flow rate was 500 sccm for both H_2 and O_2 in the OCV test. The series resistance (Rs) was determined from the high frequency intercept on the real axis of the Nyquist plot.

3. Results and discussion

All the scavengers gave acidic pH values upon dispersion in water. The pH of slurry values were 3.25, 5.35 and 5.55 for the Cr–, Mn– and Co-based scavengers, respectively. Thus, the largest acidity was observed for the sample with the highest content of sulphur moieties (Cr-sample). The occurrence of sulfonic species on the surface was identified from XPS analysis (see below).

The novel silica-supported radical scavengers based on Mn, Cr or Co oxides and containing sulfonic acid surface functionalities were characterized by X-ray diffraction (XRD) analysis (Fig. 1). In all the samples, the diffraction patterns show the presence of amorphous silica (~20° 2θ), with a broad peak that overlaps to the main signals related with the metal oxides investigated. In particular, in the pattern of the Cr-based sample no clear diffraction peak is present; whereas, for the Mn-based scavenger, the peaks related to the Miller indexes (110), (101) and (111) of the MnO_2 pyrolusite (tetragonal) structure are observed (Fig. 1). The peaks of MnO_2 were fitted to the Ref. pattern ICSD 00-001-0799. For the Co-based scavenger, the XRD analysis reveals the presence of the reflections at 18, 31, 37, 45, 59.5 and 65.6° 2θ corresponding to Co_3O_4 (the peaks were fitted to the Ref. pattern ICSD 01-080-1541). To investigate the composition of the samples, X-ray Fluorescence (XRF) was carried out. This provided information about the presence of acidic sulphur-based functionalities. The results are reported in Table 1. As observed, the composition of the various samples is not homogenous and varies with the metal involved. The uptake of metal oxide was optimized by tailoring the preparation procedure in order to have the largest amount of metal oxide, while maintaining a good dispersion on silica. The Cr-based scavenger presents the largest amount of metal (ca. 30 wt%) and sulphur (ca. 5 wt%); whereas, the Mn-based sample shows the lowest uptake both in terms of metal oxide (ca. 11 wt%) and sulphur-based functionality (0.18 wt%). An intermediate situation was observed for the Co-based scavenger in which the metal oxide uptake onto the silica support was about 25 wt% and sulphur was 0.32 wt%. Further attempts to increase the amount of Mn and Co in the samples were unsuccessful giving uneven distribution of the metal oxide onto the silica support. Thus, the samples characterized by the compositions reported in Table 1 were down-selected for further investigations.

TEM micrographs (Fig. 2) show a good distribution of the metal oxide particles onto the silica matrix (dark clusters in TEM

Table 2
Metal and sulphur loading on the surface and in the bulk of silica-supported scavengers.

Elements	Co-based scavenger		Mn-based scavenger		Cr-based scavenger	
	Surface	Bulk	Surface	Bulk	Surface	Bulk
M/Si (wt%)	1.40	32.0	0.36	12.34	4.20	44.82
S/Si (wt%)	–	0.43	–	0.20	2.0	5.24

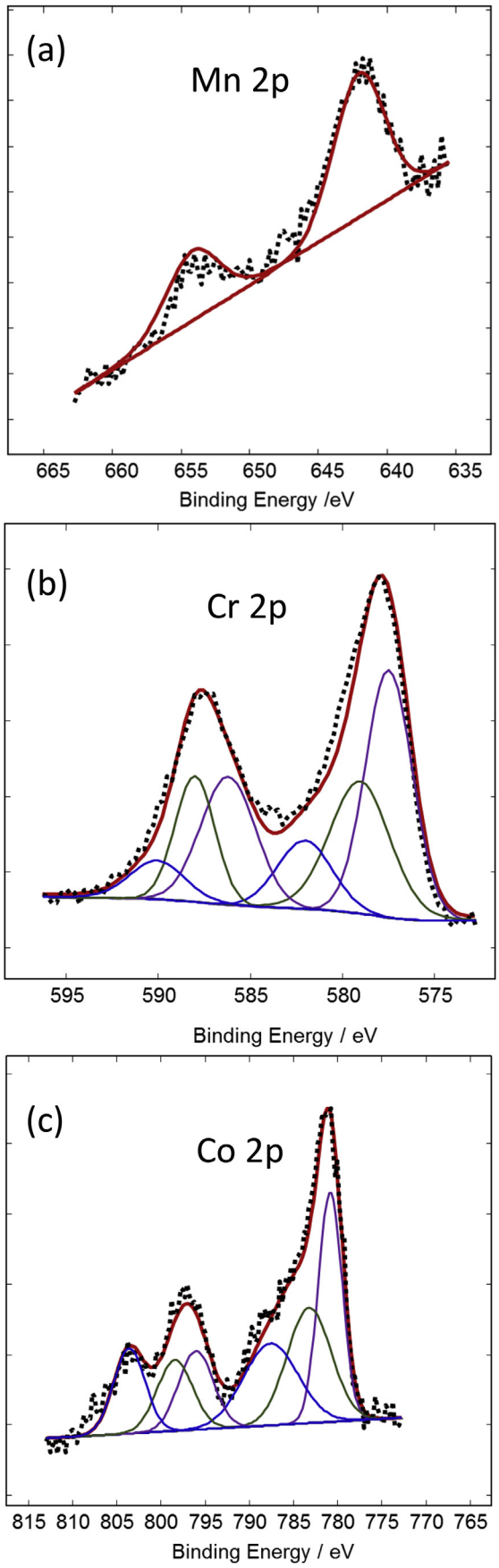

Fig. 4. XPS spectra of (a) Mn 2p, (b) Cr 2p and (c) Co 2p signals for the different scavengers.

micrographs at low magnification), although some unloaded silica is also present in particular for the Mn-scavenger (Fig. 2a). The sample based on Cr shows a high corrugation level due to the large presence of Cr-oxide (small particles, see inset in Fig. 2b) and S-based functionalities (Fig. 2b); whereas, larger particles are observed for the Co-based sample (Fig. 2c).

XPS analysis (Fig. 3) was carried out to investigate the surface composition and the oxidation state of the different oxides used as scavengers (Table 2). As can be observed from the survey spectra, the occurrence of the various transition metals on the surface is quite low. In the Mn-based sample (Fig. 4a), the surface oxidation state is corresponding to MnO_2, whereas the presence of this oxide on the surface is relatively low (M/Si ratio of 0.36%). The amount of S-based group on the surface of this sample is negligible (within the experimental error of the measurement). The scavenger containing Cr shows the largest amount of transition metal (M/Si: 4.2%) on the surface compared to the other samples and the presence of different oxidation states (Cr^{3+}, Cr^{5+}, Cr^{6+}) (Fig. 4b). In this case, the S/Si ratio is about 2%. Whereas, for the Co-based scavenger, the M/Si ratio on the surface is 1.4%; from the high resolution spectra and relative deconvolution analysis (Fig. 4c), peaks at binding energies typical of $CoSO_4$, Co_3O_4 and a shake-up line are envisaged. The metal and sulphur amount (relative to Si) on the surface and in the bulk of the scavenger are listed in Table 2; the surface loading was measured by means of XPS whereas the bulk loading was calculated as the difference between the overall composition estimated through XRF (see Table 1) and the surface abundance itself. The binding energies, the different species and their relative intensities are summarized in Table 3. The Si 2p peak was analysed to get information about the surface species occurring on the silica support for the various supported scavengers (Fig. 5). Fig. 5a shows the deconvolution peaks for the Si 2p in the Mn-based scavenger which are attributed to silanolic species (102 eV), siloxanic groups (103 eV) and Si atoms bonded to metal clusters (104 eV) through oxygen bridges. For what concerns the Cr-based scavenger (Fig. 5b), the Si 2p signal was deconvoluted in two peaks related to siloxanic groups (103 eV) and Si atoms bonded to metal clusters (104 eV). The same was found for the Si related to the Co-based scavenger (Fig. 5c), although with different relative intensities (Table 3). Fig. 6 shows the XPS spectrum of the S 2p signal in the Cr-based scavenger. The deconvolution of the S 2p signal leads to 2 peaks related mainly to acidic $-SO_3H$ groups bonded to Cr atoms (peaks at 169.83 and 167.39) with different coordination thus explaining the lowest pH value. No direct sulphonation of silica is considered since the content of sulphur moieties was relevant only in the case of the Cr-based scavenger. Thus, it is derived that sulphur species must be bonded to Cr. The binding energies are both in the range reported in the literature for sulfone-type groups bonded to clusters with different electronegativity values. For the other scavengers, the presence of S on the surface was very small to allow for a detailed analysis. Thus, the analysis and quantification of the different species were not performed.

The Fenton's test was carried out *ex-situ* in order to investigate the Fluoride Emission Rate (FER) of the scavenger-free membrane. Similar tests were made for membranes containing different metal oxides supported on silica. As clearly observed in Fig. 7, the addition of the radical scavenger, in particular the one containing Cr resulted in a great reduction in the FER which is directly related to the lower radical-triggered membrane degradation. This result is similar to the reported radical scavenging action of compounds like ceria in biological/medicinal applications [34]. As confirmed by P. Trogadas et al. [35], this effect is not due to the presence of silica, which is known to have no scavenging properties. In fact, the addition of silica particles resulted in a small but reproducible increase in FER [35]. However, silica support is necessary for both dispersion and

stabilization of the transition metal oxides, and sulphur moieties compensate for the local loss of acidity caused by the inclusion of an additive in the membrane.

Fig. 8a shows the polarization curves of membranes containing the immobilized radical scavengers having the same loading of metal, i.e. 1% mol metal/mol $-SO_3H$, compared to the bare Aquivion® PFSA membrane as the reference. The membranes were conditioned for 20 h under the following conditions: cell potential of 0.6 V, 75 °C operating temperature, 80% relative humidity (RH), using H_2/air as reactants at 1 bar absolute (barA) pressure. The performances are similar for all investigated membranes, indicating that the inclusion of the additives does not have a strong impact on the electrochemical behaviour at the beginning of life (BoL).

Membrane durability was assessed through *in-situ* AST consisting in a continuous operation under Open Circuit Voltage (OCV) (Fig. 8b). These conditions are known to enhance the deterioration of the MEA since partial pressures of the reactant gases are at their relatively maximum values, hydrogen cross-over is maximized and the high electrochemical potential of the cathode also promotes degradation of MEA components [36,37]. Recent studies [38,39] have shown that fuel cell operation at high temperature, low relative humidity, using H_2 and O_2 as reactant gases and without draining current from the system, causes an accelerated membrane degradation. For such reasons, this protocol is considered as an effective and reliable test for the evaluation of membrane durability [40,27]. The cell voltage was monitored along the test; a cut-off voltage of 0.7 V, which is typically assumed as an indication of pinholes formation in the membrane, was imposed. Scavenger-free Aquivion® PFSA-based membrane lasted in AST about 200 h whereas the same membrane containing the newly developed radical scavengers exceeded 400 h for the Co- and Mn-based samples and approached 600 h for Cr-containing scavengers. Thus, a significant increase (more than twice) in stability was recorded (Fig. 8b) with respect to the bare membrane, under same operating conditions. The Cr-scavenger-based membrane shows a better behaviour due to a larger concentration of active species on the surface of the filler as determined by XPS analysis. If we consider the ratio between the metallic concentration on the surface and in the bulk (C_{XPS}/C_{XRF}, see Table S1 of the supplementary information (SI)), we can observe that this is significantly larger for the Cr-based scavenger. All membranes have been loaded with the same amount of transition metal (bulk concentration determined by XRF), but their occurrence on the surface may vary significantly for the various scavengers. The membrane containing Cr is the one with the largest concentration of active sites on the surface, which are responsible of the scavenging properties.

As well known, transition metal ions leaching from the scavengers may have negative impact on both the ionic conductivity of the membrane and the electrodes activity. Generally, metal ion leaching occurs in the first 20–50 h of operation under OCV. Yet, in the present case, there is no significant difference in terms of high frequency resistance (Rs) for the scavenger-containing MEAs versus the reference MEA equipped with the bare membrane after 72 h of OCV test (see Table S2 of the SI). There is indeed a slight increase of Rs in the first 72 h of accelerated test, but this is similar for all MEAs including the one without scavenger. This means that the membrane is not significantly poisoned by the presence of free metal ions caused by a leaching process of the scavenger; thus, it can be stated that the leaching of ions coming from the scavengers is negligible. Another aspect that supports this evidence is the similar behaviour of the membranes containing the scavengers and the filler-free membrane during the conditioning procedure (Fig. S1 of the SI). As well known, in the case of leaching, the release of ions is higher in the first hours of MEA conditioning, in particular when humidified gases are fed, as in the present conditioning procedure. Concerning the effect on the electrode activity, polarization measurements performed after 72 h (Fig. S2 of the SI) show a similar decrease of activity in the activation region both for the MEAs based on the scavengers and the bare membrane-based MEA. Accordingly, this decay in activity can not be attributed to metal ions leaching from the scavenger since the same behaviour is observed for the scavenger-free membrane. The loss in performance is

Table 3
Binding energies related to the XPS signals, different species and their relative intensities for the different scavengers.

Elements	B.E./eV			Relative peak area/%	Species
Mn-based scavenger					
Mn	***2p*$_{3/2}$**		***2p*$_{1/2}$**		
	642.05		653.55	100	Mn^{4+} (MnO_2)
Si		***2p***			
		102.18		37.76	Si^{4+} (SiOH)
		103.11		6.36	Si^{4+} (SiOSi)
		104.36		55.88	Si^{4+} (Si bonded to metal cluster)
Cr-based scavenger					
Cr	***2p*$_{3/2}$**		***2p*$_{1/2}$**		
	577.49		586.21	49.19	Cr^{3+} ($SiOCr(OH)_2$)
	579.07		588.02	35.08	Cr^{6+} ($SiOCrOO(SO_3H)$)
	582.06		590.06	15.73	Cr^{5+} ($SiOCrO(OH)(SO_3H)$)
Si		***2p***			
		103.05		83.47	Si^{4+} (SiOSi)
		104.07		16.53	Si^{4+} (Si bonded to metal cluster)
S	***2p*$_{3/2}$**		***2p*$_{1/2}$**		
	167.62		169.39	59.07	S^{6+} ($SiOCrOO(SO_3H)$)
	169.83		171.01	40.93	S^{6+} ($SiOCrO(OH)(SO_3H)$)
Co-based scavenger					
Co	***2p*$_{3/2}$**		***2p*$_{1/2}$**		
	780.83		796.03	36.41	$Co^{2+,3+}$ (Co_3O_4)
	783.21		798.41	33.77	Co^{2+} ($CoSO_4$)
	787.58		803.58	29.82	Shake-up satellite
Si		***2p***			
		102.99		48.56	Si^{4+} (SiOSi)
		104.04		51.44	Si^{4+} (Si bonded to metal cluster)

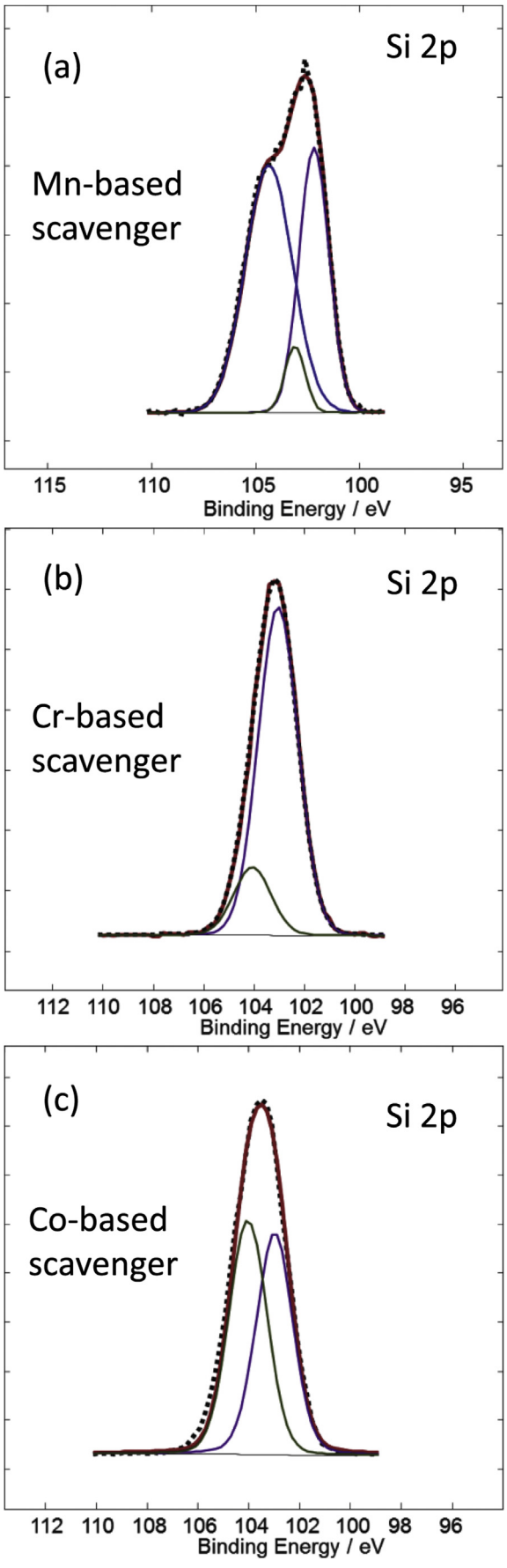

Fig. 5. XPS spectra of the Si 2p signals related to (a) Mn-based, (b) Cr-based and (c) Co-based scavengers.

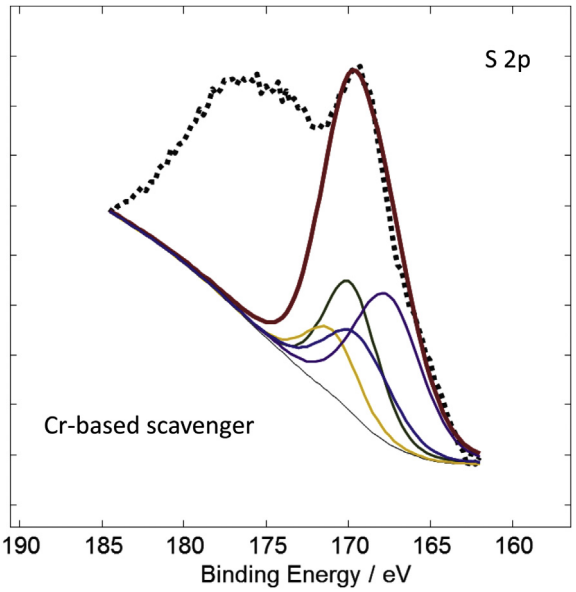

Fig. 6. Deconvoluted high resolution XPS spectrum of S 2p peak in the Cr-based scavenger.

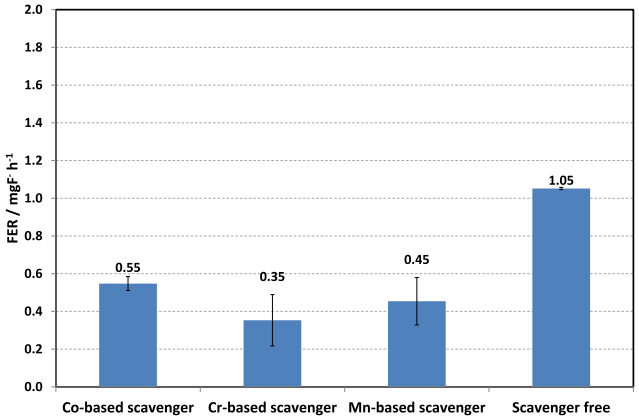

Fig. 7. Fluoride Emission Rate (FER) of membranes containing the different supported radical scavengers (1% mol metal/mol $-SO_3H$) and bare Aquivion® PFSA reinforced membrane.

attributed to carbon oxidation under OCV conditions with consequent Pt dissolution from the electrode [41]. The Pt dissolution from the catalyst layer due to carbon corrosion gives rise to membrane poisoning by Pt ions causing an increase of high frequency resistance.

4. Conclusions

Radical scavengers based on transition metal (Mn, Cr and Co) oxides supported on silica and displaying different physico-chemical properties in terms of structure, composition and morphology have been prepared following a straightforward and broadly applicable procedure. The different samples were introduced in ePTFE reinforced membranes prepared starting from commercially available and chemically stabilized Aquivion® PFSA dispersions (D79-25BS). The influence of these radical scavengers on the membrane durability was investigated *ex-situ* by using a Fenton's test and under OCV accelerated stress test in a real fuel cell. By comparing the durability of a scavenger-free Aquivion®

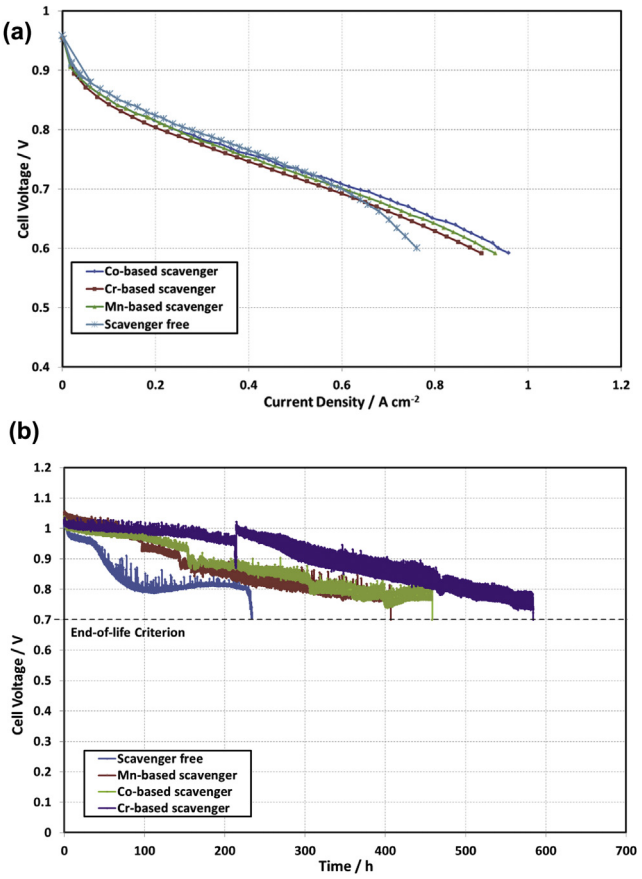

Fig. 8. (a) Polarization curves of MEAs equipped with membranes containing the immobilized radical scavengers (1% mol metal/mol $-SO_3H$) and the bare Aquivion® PFSA as reference. The polarization curves were recorded at T: 75 °C, RH: 80%, P: 1 barA, Feed: H_2/air. (b) Lifetime of scavenger free membrane (blue line) and membrane containing Mn-based (red line), Co-based (green line) and Cr-based (purple line) scavengers. Conditions: j: 0 A cm^{-2}, T: 90 °C, RH: 30%, P: 1 barA (either side), Feed: H_2 (anode)/O_2 (cathode). End-of-life limit was set at 0.7 V. (For interpretation of the references to colour in this figure legend, the reader is referred to the web version of this article.)

PFSA-based membrane with respect to the modified membranes, it results that the addition of these scavengers improves the stability of the membrane, without affecting the electrochemical performance of the fuel cell. In particular, the highly acidic and metal rich surface of the Cr-based radical scavenger seems to be strongly effective in reducing the membrane degradation and increasing its lifetime. Indeed, when compared to its scavenger-free congener, Aquivion® PFSA membrane doped with Cr-based scavenger shows a 3-fold increase in durability in AST and a 3-fold decrease in FER during Fenton's test.

Acknowledgements

The authors would like to thank Laura Molteni (Solvay Specialty Polymers) for the electrochemical characterizations.

Appendix A. Supplementary data

Supplementary data related to this article can be found at http://dx.doi.org/10.1016/j.jpowsour.2015.10.019.

References

[1] L. Carrette, K.A. Friedrich, U. Stimming, Fuel cells: principles, types, fuels, and applications, ChemPhysChem 1 (2000) 163–193.
[2] F. de Bruijn, The current status of fuel cell technology for mobile and stationary applications, Green Chem. 7 (2005) 132–150.
[3] J.A. Kerres, Development of ionomer membranes for fuel cells, J. Membr. Sci. 185 (2001) 3–27.
[4] R. Wycisk, J. Ballengee, P.N. Pintauro, Polymer membranes for fuel cells, in: E.M.V. Hoek, V.V. Tarabara (Eds.), Encyclopedia of Membrane Science and Technology, John Wiley & Sons Ltd, 2013, pp. 2033–2065.
[5] B. Smitha, S. Sridhar, A.A. Khan, Solid polymer electrolyte membranes for fuel cell applications – a review, J. Membr. Sci. 259 (2005) 10–26.
[6] F. Lufrano, V. Baglio, P. Staiti, V. Antonucci, A.S. Aricò, Performance analysis of polymer electrolyte membranes for direct methanol fuel cells, J. Power Sources 243 (2013) 519–534.
[7] H. Zhang, P.K. Shen, Recent development of polymer electrolyte membranes for fuel cells, Chem. Rev. 112 (2012) 2780–2832.
[8] M. Yoshitake, A. Watanabe, A. Perfluorinated ionic polymers for PEFCs (including supported PFSA), Adv. Polym. Sci. 215 (2008) 127–155.
[9] http://www.solvayplastics.com.
[10] J. Li, M. Pan, H. Tang, Understanding short-side-chain perfluorinated sulfonic acid and its application for high temperature polymer electrolyte membrane fuel cells, RSC Adv. 4 (2014) 3944–3965.
[11] A. Stassi, I. Gatto, E. Passalacqua, V. Antonucci, A.S. Arico, L. Merlo, C. Oldani, E. Pagano, Performance comparison of long and short-side chain perfluorosulfonic membranes for high temperature polymer electrolyte membrane fuel cell operation, J. Power Sources 196 (2011) 8925–8930.
[12] A.S. Aricò, A. Di Blasi, G. Brunaccini, F. Sergi, G. Dispenza, L. Andaloro, M. Ferraro, V. Antonucci, P. Asher, S. Buche, D. Fongalland, G.A. Hards, J.D.B. Sharman, A. Bayer, G. Heinz, N. Zandonà, R. Zuber, M. Gebert, M. Corasaniti, A. Ghielmi, D.J. Jones, High temperature operation of a solid polymer electrolyte fuel cell stack based on a new ionomer membrane, Fuel Cells 10 (2010) 1013–1023.
[13] M. Danilczuk, A.J. Perkowski, S. Schlick, Ranking the stability of perfluorinated membranes used in fuel cells to attack by hydroxyl radicals and the effect of Ce(III): a competitive kinetics approach based on spin trapping ESR, Macromolecules 43 (2010) 3352–3358.
[14] C. Lim, L. Ghassemzadeh, F. Van Hove, M. Lauritzen, J. Kolodziej, G.G. Wang, S. Holdcroft, E. Kjeang, Membrane degradation during combined chemical and mechanical accelerated stress testing of polymer electrolyte fuel cells, J. Power Sources 257 (2014) 102–110.
[15] B. Bae, K. Miyatake, M. Uchida, H. Uchida, Y. Sakiyama, T. Okanishi, M. Watanabe, Sulfonated poly(arylene ether sulfone ketone) multiblock copolymers with highly sulfonated blocks. long-term fuel cell operation and post-test analyses, ACS Appl. Mater. Interfaces 3 (2011) 2786–2793.
[16] M. Danilczuk, F.D. Coms, S. Schlick, Visualizing chemical reactions and crossover processes in a fuel cell inserted in the ESR resonator: detection by spin trapping of oxygen radicals, nafion-derived fragments, and hydrogen and deuterium atoms, J. Phys. Chem. B 113 (2009) 8031–8042.
[17] S.F. Burlatsky, V. Atrazhev, N.E. Cipollini, D.A. Condit, N. Erikhman, Aspects of PEMFC degradation, ECS Trans. 1 (2006) 239–246.
[18] A.A. Shah, T.R. Ralph, F.C. Walsh, Modeling and simulation of the degradation of perfluorinated ion-exchange membranes in PEM fuel cells fuel cells and energy conversion, J. Electrochem. Soc. 156 (2009) B465–B484.
[19] L. Ghassemzadeh, T.J. Peckham, T. Weissbach, X. Luo, S. Holdcroft, Selective formation of hydrogen and hydroxyl radicals by electron beam irradiation and their reactivity with perfluorosulfonated acid ionomer, J. Am. Chem. Soc. 135 (2013) 15923–15932.
[20] T.H. Yu, Y. Sha, W.-G. Liu, B.V. Merinov, P. Shirvanian, W.A. Goddard III, Mechanism for degradation of nafion in PEM fuel cells from quantum mechanics calculations, J. Am. Chem. Soc. 133 (2011) 19857–19863.
[21] M.P. Rodgers, L.J. Bonville, H.R. Kunz, D.K. Slattery, J.M. Fenton, Fuel cell perfluorinated sulfonic acid membrane degradation correlating accelerated stress testing and lifetime, Chem. Rev. 112 (2012) 6075–6103.
[22] B.P. Pearman, N. Mohajeri, D.K. Slattery, M.D. Hampton, S. Seal, D.A. Cullen, The chemical behavior and degradation mitigation effect of cerium oxide nanoparticles in perfluorosulfonic acid polymer electrolyte membranes, Polym. Degrad. Stab. 98 (2013) 1766–1772.
[23] Z. Wang, H. Tang, H. Zhang, M. Lei, R. Chen, P. Xiao, M. Pan, Synthesis of Nafion/CeO_2 hybrid for chemically durable proton exchange membrane of fuel cell, J. Membr. Sci. 421–422 (2012) 201–210.
[24] P. Trogadas, J. Parrondo, V. Ramani, Degradation mitigation in PEM fuel cells using metal nanoparticle and metal oxide additives, in: Q. Wang, L. Zhu (Eds.), Functional Polymer Nanocomposites for Energy Storage and Conversion, ACS Symposium Series; American Chemical Society, Washington, DC, 2010, pp. 187–207.
[25] P. Trogadas, J. Parrondo, V. Ramani, CeO_2 surface oxygen vacancy concentration governs in situ free radical scavenging efficacy in polymer electrolytes, ACS Appl. Mater. Interfaces 4 (2012) 5098–5102.
[26] F.D. Coms, H. Liu, J.E. Owejan, Mitigation of perfluorosulfonic acid membrane chemical degradation using cerium and manganese ions, ECS Trans. 16 (2008) 1735–1747.
[27] E. Endoh, S. Terazono, H. Widjaja, Y. Takimoto, Degradation study of MEA for

PEMFCs under low humidity conditions, Electrochem. Solid State Lett. 7 (2004) A209–A211.
[28] C. D'Urso, C. Oldani, V. Baglio, L. Merlo, A.S. Aricò, Towards fuel cell membranes with improved lifetime: Aquivion® perfluorosulfonic acid membranes containing immobilized radical scavengers, J. Power Sources 272 (2014) 753–758.
[29] M. Watanabe, H. Uchida, Y. Seki, M. Emori, P. Stonehart, Self-humidifying polymer electrolyte membranes for fuel cells, J. Electrochem. Soc. 143 (1996) 3847–3852.
[30] A.S. Aricò, P. Cretì, P.L. Antonucci, V. Antonucci, Comparison of ethanol and methanol oxidation in a liquid-feed solid polymer electrolyte fuel cell at high temperature, Electrochem. Solid State Lett. 1 (1998) 66–68.
[31] A. Di Blasi, V. Baglio, A. Stassi, C. D'Urso, V. Antonucci, A.S. Aricò, Composite polymer electrolyte for direct ethanol fuel cell application, ECS Trans. 3 (2006) 1317–1323.
[32] M.A. Harmer, W.E. Farneth, Q. Sun, High surface area Nafion resin/silica nanocomposites; a new class of solid acid catalyst, J. Am. Chem. Soc. 118 (1996) 7708–7715.
[33] W. Fang, S. Wang, A. Liebens, F. De Campo, H. Xu, W. Shei, M. Pera-Titus, J.-M. Clacens, Silica-immobilized Aquivion PFSA Superacid: application to heterogeneous direct etherification of glycerol with n-butanol, Catal. Sci. Technol. 5 (2015) 3980–3990.
[34] S. Babu, A. Velez, K. Wozniak, J. Szydlowska, S. Seal, Electron paramagnetic study on radical scavenging properties of ceria nanoparticles, Chem. Phys. Lett. 442 (2007) 405–408.
[35] P. Trogadas, J. Parrondo, V. Ramani, Degradation mitigation in polymer electrolyte membranes using cerium oxide as a regenerative free-radical scavenger, Electrochem. Solid State Lett. 11 (2008) B113–B116.
[36] S. Kundu, M. Fowler, L.C. Simon, R. Abouatallah, Reversible and irreversible degradation in fuel cells during open circuit voltage durability testing, J. Power Sources 182 (2008) 254–258.
[37] K. Teranishi, K. Kawata, S. Tsushima, S. Hirai, Degradation mechanism of PEMFC under open circuit operation, Electrochem. Solid State Lett. 9 (2006) A475–A477.
[38] A.C. Fernandes, E.A. Ticianelli, A performance and degradation study of Nafion 212 membrane for proton exchange membrane fuel cells, J. Power Sources 193 (2009) 547–554.
[39] Y.-H. Lai, G.W. Fly, In-situ diagnostics and degradation mapping of a mixed-mode accelerated stress test for proton exchange membranes, J. Power Sources 274 (2015) 1162–1172.
[40] V.O. Mittal, H.R. Kunz, J.M. Fenton, Effect of catalyst properties on membrane degradation rate and the underlying degradation mechanism in PEMFCs, J. Electrochem. Soc. 153 (2006) A1755–A1759.
[41] A.S. Aricò, A. Stassi, E. Modica, R. Ornelas, I. Gatto, E. Passalacqua, V. Antonucci, Performance and degradation of high temperature polymer electrolyte fuel cell catalysts, J. Power Sources 178 (2008) 525–536.